THE DYNAMICS OF SLACK MARINE CABLES

O.M. Griffin and F. Rosenthal

Marine Technology Division
Naval Research Laboratory

Naval Research Laboratory
Washington, DC 20375

TABLE OF CONTENTS

THE DYNAMICS OF SLACK MARINE CABLES

1. INTRODUCTION

Cables are employed in a wide variety of marine and offshore operations. Common examples include moorings, power supply, salvage operations and umbilicals. Most of the computer models developed to date assume that the tension in the cable elements is above a threshold level such that the vibrational behavior of the cable is essentially that of a taut string. For many applications in which catenary effects are important, and umbilical applications where the cable tension may be required to be small, a significant amount of cable slack may be realized. Examples of slack cable applications include deep water moorings, horizontal cable segments between vertical legs of a cable array. the downstream vertical leg of a multiple-leg cable array, and guy lines of deep water guyed towers and semi-submersible platforms. Design analysis of cable structures such as these using conventional taut cable techniques could lead to incorrect conclusions and to inappropriate selection of the required cables.

The purpose of this report is to discuss the present state-of-the-art for the analysis and modelling of slack marine cables. A summary is given of the linear theory for the vibration of horizontal and inclined slack cables and the important differences between the two cases are pointed out. Examples are given of the numerical results which can be obtained with available codes for computing the dynamics of slack cables with and without attached arrays of discrete masses.

Finally, recommendations are made for the further development of suitable slack cable computer codes for use in engineering practice. The approach to the problem is expected to be analogous to that taken in developing and verifying experimentally a computer code for predicting the vibration response of taut marine cables with attached discrete masses (Sergev and Iwan, 1980: Griffin and Vandiver, 1983: Iwan and Jones, 1984).

2. RELATED INVESTIGATIONS

The taut cable or wire was one of the first structural systems to be studied, as early as the eighteenth century. In most engineering applications cables exhibit finite sag to some degree. This led Rohrs (1851) and then Routh (1868) to develop solutions for the dynamics of an inextensible chain suspended between two points at the same elevation. Later, Saxon and Cahn (1953) developed an asymptotic solution for the inextensible chain which was in good agreement

with the derivation of Pugsley (1949) and experimental data. An excellent historical discussion of the problem is given by Irvine (1981).

The earliest solutions of the inelastic chain problem were not able to reproduce the results for a taut cable. Several investigators showed that the inclusion of elasticity effects can join the taut wire and inelastic chain regimes and provide solutions for intermediate conditions: for example, Soler (1970) and Simpson (1966). It was Irvine and Caughey (1974) who provided an extensive study of the linear cable dynamics and offered a clear physical understanding of the phenomenon. Their solution reproduced both the inelastic chain and the taut wire results for a cable suspended between two points at the same elevation. An intermediate range was found, for sag-to-span ratios below 1:8, over which the natural frequencies of the symmetric cable modes, i.e. symmetric relative to a vertical line passing through the cable midpoint, were between those of a taut cable and an inextensible cable. A fundamental parameter was identified which governed the extensible cable dynamics and accounted for both elasticity and the equilibrium geometry of the cable.

Soon after the work reported by Irvine and Caughey, several additional numerical and analytical studies were made of the slack cable dynamics. Numerical computations of the cable natural frequencies and mode shapes using a discretized cable model were reported by West, Geschwindner and Suhoski (1975).

Somewhat later Henghold, Russell and Morgan (1977) followed with a finite-element numerical model for a cable in three dimensions. The computations by West et al were limited to a cable with ends at the same elevation, while the results reported by Henghold et al applied to the more general case of both horizontal and inclined cable spans. Both of these numerical studies were limited to the lower cable modes because of the relatively small number of cable segments that were employed. West, Suhoski and Geschwindner (1984) recently have applied their method to the dynamics of the suspension bridge. Many features of the slack cable dynamics, including the frequency crossover described below for the horizontal cable, were observed for the case of the suspension bridge under certain conditions.

A finite-element model for the dynamics of sagged cables was developed by Gambhir and Batchelor (1978). Both two-dimensional and three-dimensional computer codes were developed using curved and straight finite elements for the general case of a cable with end points at different elevations. A comparison was made with the numerical results of West el al (1975) and the previous work of Saxon and Cahn (1953) and of Pugsley (1949). Good agreement was found overall and the finite element method showed excellent covergence characteristics relative to other numerical approaches.

A more recent numerical study of the dynamics of slack cables with and without attached masses was conducted by

Rosenthal (1981). This approach is based upon Stodola's method for the dynamics, which is a successive approximation approach to computing the natural frequencies and mode shapes of the cable. One example based upon a relatively small number of ten cable integration intervals caused inaccuracies to appear in the higher-mode natural frequencies. The computations were made for the purpose of comparing with the results of Henghold et al who used fourteen elements. However, it also was shown that large numbers of integration intervals (up to 60) could be used conveniently. This was necessary when numerous masses were attached to the cable and/or the higher mode frequencies were required.

Ramberg and Griffin (1977) measured the natural frequencies of taut and slack marine cables in air and in water and obtained good agreement with predictions based upon the linear theory of Irvine and Caughey. Soon after, Irvine (1978) extended his linear theory to the more general case of an inclined slack cable. Ramberg and Bartholomew (1982) again obtained good agreement between their measured natural frequencies of inclined cables and those predicted using Irvine's linear theory. However, as discussed below, Irvine's theory for the horizontal cable cannot be extended to inclined cables except under special circumstances.

All of these recent studies suggested the existence of a frequency crossover phenomenon which appears in the transitional

regime where neither the inextensible cable results nor the taut cable results are appropriate by themselves. At the apparent frequency crossover three modes of the cable have the same natural frequency. These modes include a symmetric in-plane mode, an antisymmetric in-plane mode and an out-of-plane or sway mode. The symmetric modes contain an even number of nodal points along the cable while the anti-symmetric modes contain an odd number of nodes.

The problem of the inclined cable has been investigated most recently by Triantafyllou and Bliek (1983) and by Triantafyllou (1984). The analysis is based on a WKB-type asymptotic solution for the cable dynamics. For the special case of a horizontal cable the method reduces to all of the previous known solutions described above. However, there are some important differences in the case of an inclined cable. Two distinct physical mechanisms of vibration were identified. These correspond to the transverse and longitudinal or elastic waves in the case of the taut cable. As the curvature (sag) of the cable increases, modes develop which are hybrid in character (neither symmetric nor antisymmetric). This phenomenon is characterized by a shift of the natural frequency of a symmetric mode toward the natural frequency of an antisymmetric mode, but no crossover occurs. Instead the two modes become distinct again and the eigenvalues of the symmetric mode lie on the continuation of the eigenvalues of the antisymmetric mode (from before the hybrid modes occurred)

and vice versa. However, only the mode shape variation is changed. The natural frequencies for the inclined cable computed by Triantafyllou and Bliek were virtually identical to those given by Irvine (1981).

3. THE LINEAR THEORY FOR A HORIZONTAL SLACK CABLE

The vibrations of taut cables are described appropriately by the classical taut string equations. This approach neglects the cable's bending stiffness and finite-amplitude vibration effects, but it is accurate to within 2-4 percent for many cables over a wide range of conditions. As the tension is relaxed, a cable eventually assumes the configuration shown in Fig. 1. H is the horizontal component of tension at the supports and each vertical component V is equal to half ot the total cable weight. The limiting sag-to-span ratio $s/\ell \rightarrow 0$ is accompanied by $H \approx T$ since the cable weight becomes a negligible fraction of the tension. At the other extreme, when s/ℓ becomes large, V is comparable to or larger than H and the cable assumes a classical catenary shape. The natural vibrations of catenaries are known for $s/\ell >$ 1:1.0, but until recently they could not be reconciled with the taut string theory as the ratio of sag-to-span vanished. This difficulty was overcome by Irvine and Caughey (1974) and some others preceding them by including the extensional behavior of the cable in the theory for horizontal cables. The comparable theoretical development for an inclined cable has been studied by
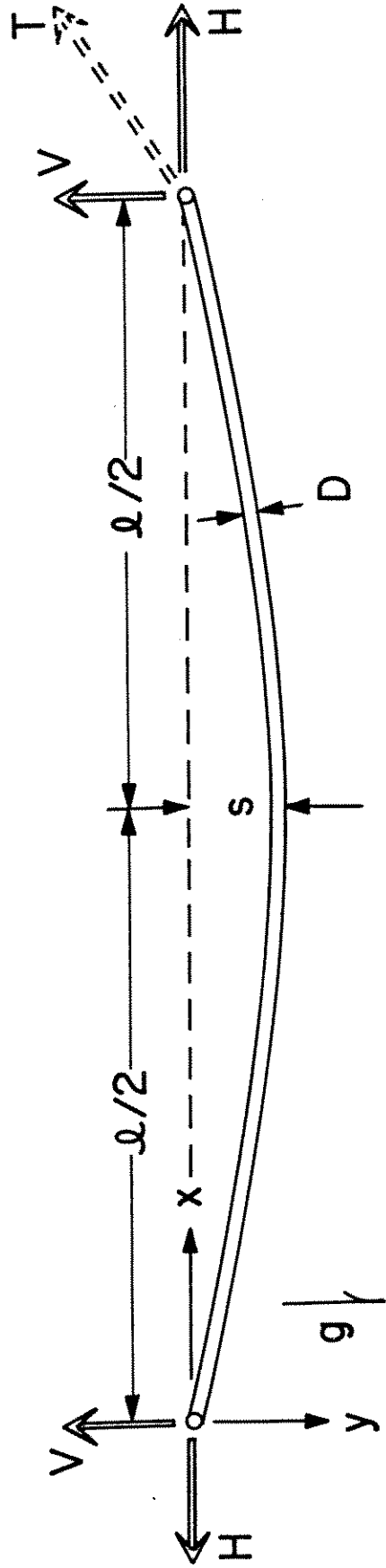
Figure 1 — The geometry and nomenclature for a slack cable of
length L, span ℓ, and mass per unit length m.

Irvine (1978, 1981) and by Triantafyllou and Bliek (1983), Triantafyllou (1984b), and Bliek (1984).

A summary is given here of Irvine and Caughey's development for a cable with end points at the same elevation, and the results applicable to marine cables are discussed. The equilibrium shape of an inextensible cable is given by

$$y = \frac{mg\ell^2}{2H} \left(\frac{x}{\ell} - \left(\frac{x}{\ell} \right)^2 \right) \tag{1}$$

for $d/\ell < 1:8$ and where $d = mg\ell^2/8H$ is the midspan sag. As we shall see later in the report, this is a special case of the general extensible cable dynamics problem. The length of this cable is

$$L \approx \ell \left(1 + \frac{8}{3} \left(\frac{d}{\ell} \right)^2 \right) ,$$

so that if three of the quantities mg, H, d, ℓ and L are known then the other two can be found. However, owing to stretch, the sag and length of a real cable are greater than the inextensible values while the horizontal component of tension of the stretched cable is less. If this new sag is s while the new horizontal component of tension is $(H - \Delta H)$, then equilibrium dictates that

$$\frac{s - d}{d} = \frac{H*}{1 - H*} \tag{2}$$

where $H* = \Delta H/H$. Compatibility of the cable displacement requires, in addition, that

$$(1 - H*)^3 = \frac{\lambda^2}{24} (2H* - H*^2) \tag{3}$$

where

$$\lambda^2 = \left(\frac{mg\ell}{H}\right)^2 \frac{\ell}{\left(\frac{HL_e}{EA}\right)} = 64 \left(\frac{d}{\ell}\right)^2 \frac{\ell}{\left(\frac{HL_e}{EA}\right)} \tag{4}$$

and

$$L_e = \int_0^\ell \left(1 + \left(\frac{dy}{dx}\right)^2\right)^{3/2} dx \approx 1 \left(1 + 8 \left(\frac{d}{\ell}\right)^2\right) \tag{5}$$

The quantity EA is the product of the elastic modulus and the cross-sectional area of the cable, while L_e, the "virtual" cable length, essentially is the stretched cable length correct to the order of the linear theory approximation. As noted by Irvine and Caughey, the dimensionless variable λ^2 is the fundamental parameter of the extensible cable because it accounts for both the elasticity and equilibrium geometry of the cable. In the subsequent notation H will be taken to mean the horizontal component of tension in the extensible cable profile, i.e. the measured tension.

In the study of natural vibrations, the equations of motion can be linearized about the equilibrium configuration. Then the

out-of-plane motions are decoupled to first order and the remaining in-plane modes fall into two classes. In the first class there were thought to be no first-order tension fluctuations induced at the supports; only the second class was thought to induce such fluctuations. The two cases were characterized respectively by mode shape symmetry and antisymmetry about the cable midpoint. The antisymmetric motions of the sagging cable have the same frequency equation as the taut string, but the symmetric modes obey a different eigenvalue equation. This means that the classical equation for a taut cable is valid for $0 <$ $s/\ell < 1:8$ if n is even, whereas the symmetric mode frequencies are given by

$$\tan \left(\frac{\beta\ell}{2}\right) = \frac{\beta\ell}{2} - \frac{4}{\lambda^2} \left(\frac{\beta\ell}{2}\right)^3 , \tag{6}$$

where

$$\beta = \left(\frac{m \, \omega^2}{H}\right)^{1/2} . \tag{7}$$

The result simplifies to the taut cable equation in the limit $s/\ell = 0$ when $mg\ell \ll H$ in Eq. (4). In that case λ^2 approaches zero and equation (4) reduces to

$$\lim_{s/\ell \to 0} \left[\tan \frac{\beta\ell}{2}\right] = -\infty \tag{8}$$

and

$$(\beta\ell)_k = (2k - 1) \pi , \quad k = 1,2,3... \tag{9}$$

or

$$f_n = \frac{n}{2\ell} \sqrt{\frac{T}{m}}, \text{ n odd .} \tag{10}$$

A graphical solution to Eq. (6) is presented in Fig. 2 for several values of the parameter λ^2. The arrows indicate the values of $\frac{\beta\ell}{2}$ which correspond to the natural frequencies of a taut string. For small λ^2 the symmetric mode frequencies approach those of a taut string. As λ^2 increases, the first symmetric mode frequency increases toward the first antisymmetric frequency. They coincide for $\lambda^2 = 4\pi^2$ and thereafter the first symmetric mode frequency is greater than the higher antisymmetric frequencies. At still larger values of λ^2 these frequency crossovers occur at the higher symmetric modes.

As an example consider $\lambda^2 = 36\pi^2$. The antisymmetric mode values of $\frac{\beta\ell}{2}$ are given by $\frac{n\pi}{2}$, n = 2,4,6, etc. as before while the first four symmetric mode solutions are indicated by the encircled intersections in Fig. 2. The lowest two symmetric mode frequencies have crossed over and lie above the lowest two antisymmetric frequencies. The frequencies of the third sym- metric and antisymmetric modes are equal (crossover is occuring) while the fourth symmetric mode frequency is quite close to the n = 7 frequency of a string. For the modes higher than n = 7 the natural frequencies are essentially those of the taut string. The catenary effects progress into the higher modes as λ^2

increases, but for finite λ^2 some unaffected modes remain. Returning to the first symmetric mode frequency of the example, there is little difference between $\lambda^2 = 36\pi^2$ and $\lambda^2 = \infty$ so that the first mode is nearly inextensible. For $\lambda^2 \rightarrow \infty$, Eq. (6) reduces to

$$\tan \left(\frac{\beta\ell}{2}\right) = \left(\frac{\beta\ell}{2}\right) \qquad\qquad (11)$$

which is also plotted in Fig. 2. With this frequency equation the symmetric natural frequencies are again well ordered and alternate with antisymmetric frequencies, but there is a shift of between $0.93\,\pi$ and π in these symmetric mode frequencies with respect to the taut string symmetric mode frequencies.

The mode shapes of a horizontal slack cable are affected by the apparent frequency crossover in a complex manner. A symmetric mode must possess an even number of nodes. Thus the mode shape acquires two additional nodes in crossing over, and alters its overall form while preserving symmetry. The transition is smooth as shown in Fig. 3 which is adapted from a related numerical simulation by West, Geschwindner and Suhoski (1975). A dashed line which corresponds to the example $\lambda^2 = 36\pi^2$ is included in Fig. 3(a). The related but more complex case of an inclined slack cable is considered later in the report.

This section has summarized the linear solution derived by Irvine and Caughey (1974) for the dynamics of slack cables with
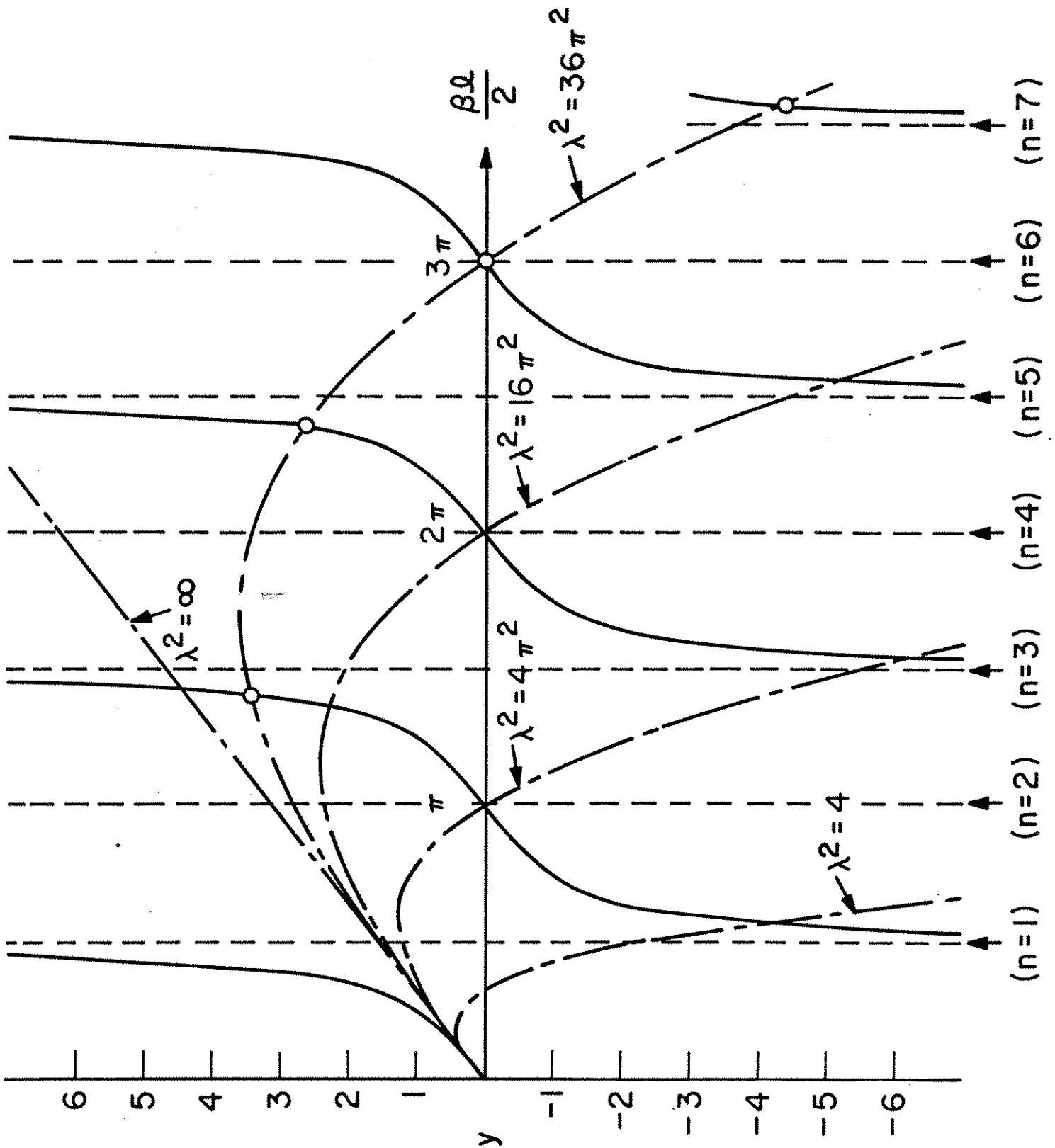
Figure 2 – Graphical solutions to Eq. (6) for the lowest symmetric-mode natural frequencies of a flat-sag cable, from Ramberg and Griffin (1977). The effects of cable sag and extension are included in the parameter λ^2 (see Eq. (4)). For $\lambda^2 \to \infty$ the cable is inextensible, and for $\lambda^2 = 0$ the cable is taut.
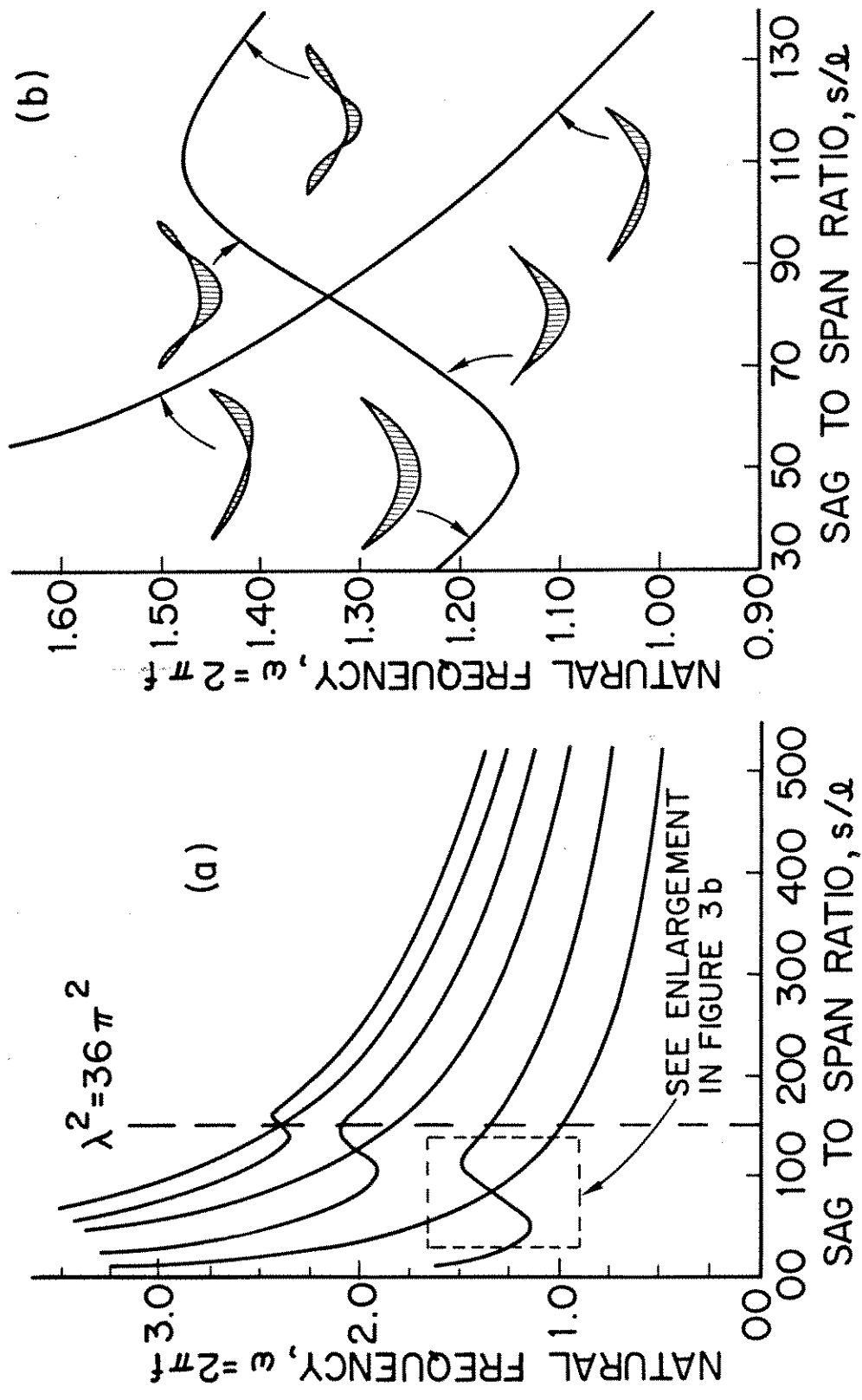
Figure 3 - Two figures adapted from West et al (1975) showing (a) the natural frequencies versus the variation in sag including modal crossovers for a cable with its ends at the same elevation, and (b) an indication of the mode shape transitions during a crossover of the lowest modes of Figure 3(a).

sag-to-span ratios of 1:8 or less. This is a special case of the more general asymptotic perturbation solution for the linear dynamics of taut and slack cables derived by Triantafyllou (1984b), and discussed further by Bliek (1984).

4. THE ONSET OF CATENARY EFFECTS

An expression for the "critical" tension corresponding to the onset of catenary behavior in a horizontal cable can be obtained from Eq. (4). The result is

$$H_{crit} = \left(\frac{mg}{\lambda_{crit}}\right)^{2/3} \left(\frac{EA}{L_e}\right)^{1/3} \ell . \tag{12}$$

By requiring the cable frequency to be within 5 percent of the taut string value, an approximation consistent with the accuracy of the string equation, one obtains

$$\lambda^2_{crit} = 1.26 \tag{13}$$

Since $d \approx s$ for typical cables when λ^2 is small, Eq. (5) becomes

$$L_e = \ell \left(1 + 8 (s/\ell)^2\right) < 9\ell/8 . \tag{14}$$

The onset of slack effects occurs near the limit of $s/\ell \rightarrow 0$, so that a slightly conservative estimate is established by $L_e \approx \ell$ to obtain

$$H_{crit} = 0.93(W^2\,EA)^{1/3}\ ,\qquad\qquad (15)$$

where $W = mg\ell$ is the total weight of the cable to the accuracy of the linear theory. The corresponding critical sag is

$$s_{crit} = 0.134\left(\frac{W}{EA}\right)^{1/3}\ell\ .\qquad\qquad (16)$$

It should be emphasized that this criterion applies to the initiation of catenary effects in only the symmetric modes, since the antisymmetric modes are unaffected for $s/\ell < 1:8$ and $H > W$. Furthermore, at $H = H_{crit}$ the only affected mode will be the $n = 1$ mode. If one is interested in the onset of slack effects in the higher symmetric modes, then the expression becomes

$$H_{crit} = \left(\frac{W^2\,EA}{\lambda_n^2}\right)^{1/3}\qquad\qquad (17a)$$

$$\lambda_n^2 = \frac{4\ \alpha^3}{\alpha - \tan\alpha},\ \alpha = 0.525\ n\ \pi,\ n = 1,3,5,\ \text{etc.}\qquad (17b)$$

Experimental results are discussed later in this report and in a previous related paper and report which deal with marine cable applications; see Ramberg and Griffin (1977), Griffin et al (1981).

5. THE INCLINED SLACK CABLE

The linear theory just described has proven to be a valuable tool in the analysis of marine cable vibrations. A shortcoming

of the original analysis of Irvine and Caughey was a restriction to horizontal cables or, more precisely, to cables with supports at the same elevation. One simple way to extend this linear theory to cables with inclined chords is to view the cable in a coordinate system inclined with the cable (Irvine, 1978). In order to retain symmetry about the cable midpoint, an essential feature of the linear analysis, one must ignore the effect of the chordwise component of gravity. Essentially it is assumed that the static configuration of the cable is parabolic. The problem then reduces to the previous analysis except that the weight per unit length is given by $w = mg \cos \theta$ where θ is the chord inclination angle from the horizontal. The analysis of Irvine and Caughey (1974, 1978) for the parabolic cable (horizontal and inclined) was continued more recently by Veletsos and Darbre (1983).

According to the linear theory, the horizontal (or chordwise) component of tension H is constant along the cable,

$$H = mg \cos \theta \ell^2 / 8s \ .\qquad(18)$$

It should be noted that ℓ now is the horizontal component of the distance (chord) between the cable supports. However, the chordwise component of gravity produces a change in H from one end to the other of an inclined cable by an increment ΔH given by

$$\Delta H = mg \ell \sin \theta \ . \tag{19}$$

Thus the modified linear analysis for inclinded slack cables is subject to

$$\varepsilon = \frac{\Delta H}{H} \ll 1$$

or

$$\varepsilon = 8 s \tan \theta / \ell \ll 1 \ . \tag{20}$$

This condition places rather stringent limits on the sag-to-span ratio as the chord inclination angle steepens.

Triantafyllou (1984b) Triantafyllou and Bliek (1983), and Bliek (1984) have developed asymptotic analytical solutions based upon perturbation theory for the linear dynamics of taut and sagged inclined cables. It was found from the analysis that the most important parameter governing the cable dynamics was

$$Q(S) = - \frac{m}{M} \alpha_0^2 \left(1 - \frac{m \ \omega^2}{EA \ \alpha_0^2(S)} \right) \tag{21}$$

where $\alpha_0 = \dfrac{d\phi_0(S)}{dS}$, the local curvature, and M is the virtual (physical + added) mass of the cable. The parameter Q represents the interaction between and relative importance of elasticity and curvature effects for the inclined cable. The linear theory developed by Irvine and Caughey (1974, 1978) for horizontal and inclined cables represents the special case Q = constant. This

is the parabolic cable approximation, or α_0 = constant together with the condition that the ratio of cable weight to tension, $mg\ell/H_1$, is small. The solution obtained by Triantafyllou consists of slow and fast varying terms with respect to the distance along the cable. When $Q(S)$ becomes zero at some point along the cable, the slowly varying solution is of exponential form up to the $Q = 0$ point and sinusoidal beyond it. This transition corresponds to a change from inextensible cable dynamics (exponential; curvature important) to taut cable dynamics (sinusoidal; elasticity important). Over some length of the cable there will be in general a combination of the two types of behavior.

A frequency crossover never occurs in the case of the inclined cable. Instead the modes are hybrid in form over the transition range from the inextensible to the taut cable. They are a mixture of symmetric and antisymmetric modes as shown by Triantafyllou (1984b). There is virtually no difference in the natural frequencies computed by the methods developed by Triantafyllou and by Irvine (1978), as shown in Table 1, but the hybrid mode shapes are unique in form as shown here in an example given below.

The governing parameter λ^2 for the inclined cable is given by (see Irvine, 1978)

$$\lambda_1^2 = \left(\frac{mg\ell\cos\theta}{H_1}\right)^2 \ell_1 / \left(\frac{H_1 L_{e1}}{EA}\right), \qquad (22)$$

TABLE 1

Natural Frequencies of Taut and Slack Inclined Cables
(from Triantafyllou, 1984b)

	ω_1	ω_2	ω_3	ω_4	ω_5
Triantafyllou, 1984b	2.15	2.21	3.38	4.37	5.48
Irvine, 1978	2.17	2.20	3.39	4.39	5.51

Cable Properties:

Length (unstretched), L = 330m

Cross section, $A = 7.07 \ (10^{-4}) \ m^2$

Young's modulus, $E = 15 \ (10^{10}) \ N/m^2$

Mass per unit length, m = 5.56 kg/m

Weight per unit length (in water), w = 47.6 N/m

Added mass coefficient = 0.128

Water Depth, D = 130m

Horizontal force on top = 76,300 N

Tension on top, T = 86,660 N

Inclination angle, $\phi_a = 23.46°$

Curvature at the midpoint, $\alpha_1 = 5.24^* 10^{-4}$

Nondimensional Quantities:

$$\frac{WL}{T_a} = 0.18 = 1.8 \ \varepsilon$$

$$L\alpha_1 = 0.173 = 1.73 \ \varepsilon$$

$$\frac{T_a}{EA} = 8.17 \ (10^{-4}) = 0.817 \ \varepsilon^3$$

$$\frac{\omega_{2n}^2 L}{g} \simeq n^2 \ 162 = 1.62 \ n^2/\varepsilon^2$$

$$\varepsilon = 0.1$$

where $H_1 = H/\cos\theta$, $\ell_1 = \ell/\cos\theta$ and $L_{e1} = L_e/\cos\theta$. There is a direct relationship between the parameters λ^2 and Q. This is readily shown for a shallow-sag horizontal cable as was done by Triantafyllou. When the natural frequencies of an inclined cable (properties given by Triantafyllou, 1984b) are plotted against λ_1^2, the results are as shown in Fig. 4. There is no crossover but instead the two natural frequency curves pass close together. The transitions of the first two modes for $\theta = 60^0$ and $mgL/H_1 = 0.15$ are shown in Fig. 5. Well below the transition the mode shapes are those of a taut cable. Then the symmetric and anti-symmetric modes become hybrid modes. Above the transition region, the lower hybrid mode which originated from the symmetric mode becomes antisymmetric, and the other hybrid mode is trans-formed into the first symmetric mode of an inextensible cable. The extent of the transition region is dependent on the elastic strain H_1/EA. As noted by Bliek, previous investigators, e.g. Irvine (1978), Henghold et al (1977), as a practical matter were unable to observe the hybrid mode behavior because of the small transition region which was produced by the cable parameters in those studies.

The critical <u>total</u> tension H_1 can be defined for an inclined slack cable in much the same way as was done for a cable with supports at the same elevation. For the inclined cable.
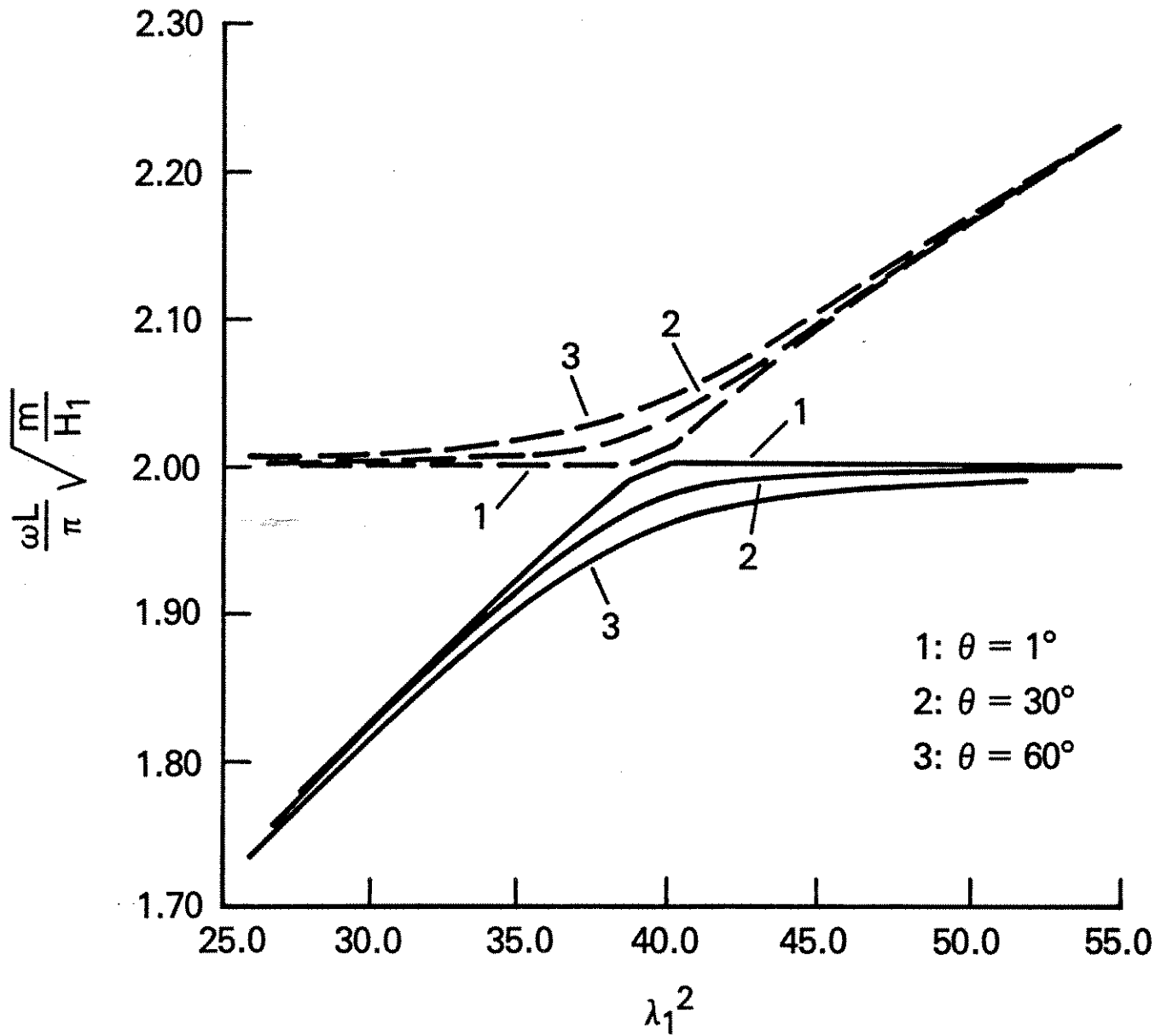
Figure 4 - The first two natural frequencies of an inclined slack
cable in air versus the parameter λ_1^2, for $mgL/H_1 = 0.15$ and for
inclination angles of $\theta = 1^0$, 30^0 and 60^0: from Triantafyllou
(1984b).

MODE 1   MODE 2

$\lambda_1^2 = 7.4$

SYMMETRIC   ANTISYMMETRIC
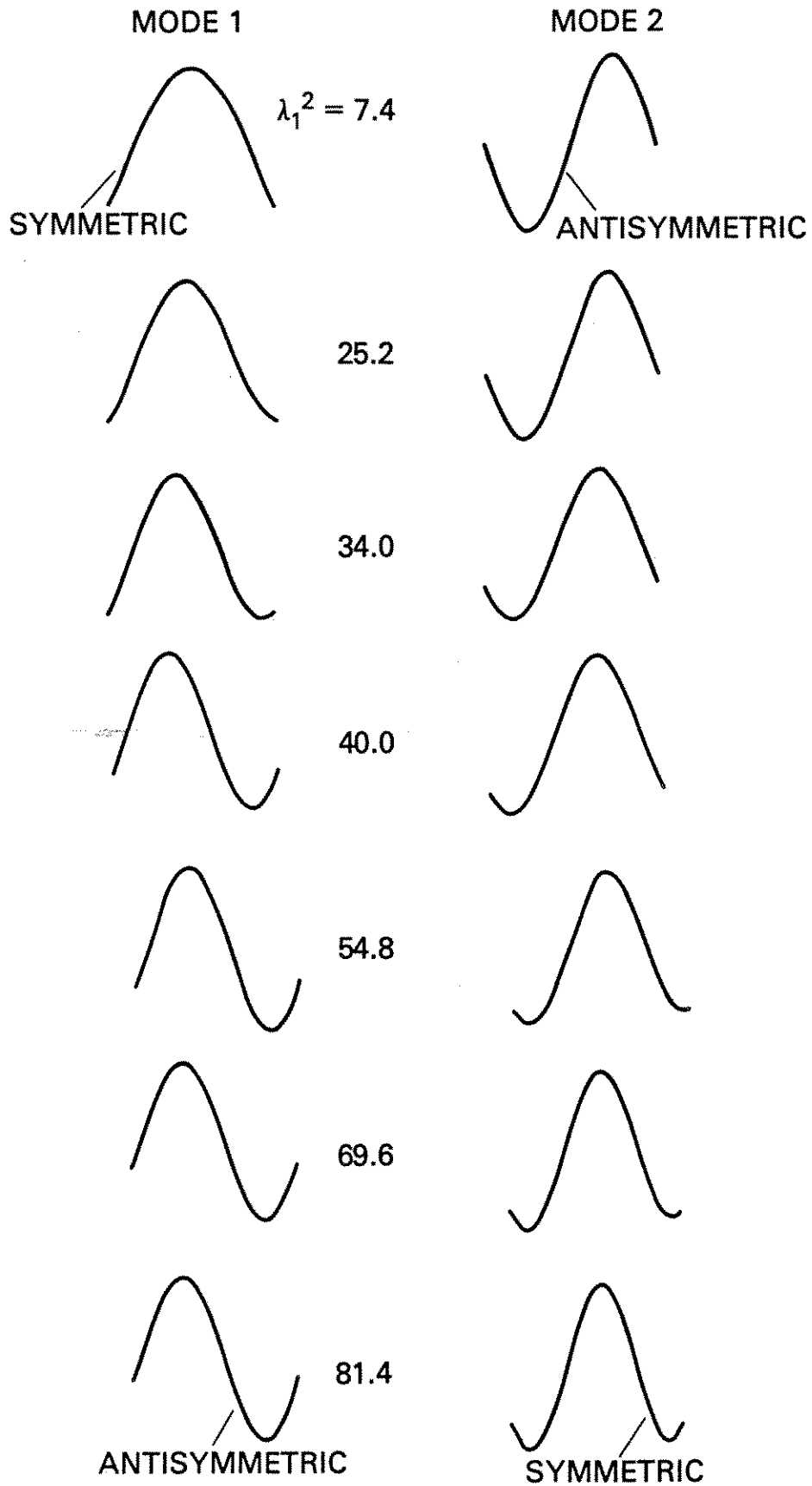
25.2

34.0

40.0

54.8

69.6

81.4

ANTISYMMETRIC   SYMMETRIC

Figure 5 — The transition with increasing λ_1^2 of the first two natural modes of an inclined slack cable in air, for $\theta = 60^0$ and $mgL/H_1 = 0.15$ as in Figure 4; from Triantafyllou (1984b).

$$\lambda_1^2 = \left(\frac{mg\ell_1}{H_1}\cos^2\theta\right)^2 \ell_1\left(\frac{EA}{H_1 L_{e1}}\right), \qquad (23)$$

and if the assumption once again is made that $L_{e1} \approx \ell_1$, then

$$\lambda_1^2 = \left(\frac{mg\ell_1}{H_1}\right)^2 \left(\frac{EA}{H_1}\right)\cos^2\theta .$$

This equation can be rearranged into the form

$$H_1^3 = \frac{1}{\lambda_1^2}\left(mg\ell_1\right)^2 EA \cos^2\theta \qquad (23a)$$

which becomes

$$\cos^{2/3}\theta$$

$$H_1 = 0.93 \; \overset{\nearrow}{\cos^2\theta} \left(W_1^2 EA\right)^{1/3} \qquad (24)$$

since $W = mg\ell_1$, is the <u>total</u> cable weight to the accuracy of the linear theory and again $\lambda_1^2 = 1.26$ for the lowest symmetric (n=1) cable mode. The antisymmetric modes are unaffected as before for $s/\ell < 1:8$ and $H_1 > W_1$. The onset of slack effects in the higher cables can be estimated by using Eq. (17b) to compute $\lambda_{1,n}^2$.

A major finding of the studies by Triantafyllou and Bliek (1983, 1984, 1984b) is that the dynamic tension in the cable is increased greatly over the hybrid mode transition range. Previously, dynamic tension effects were thought to be minimal for the antisymmetric modes, so that from a practical standpoint

fatigue and failure effects were only important for the symmetric modes.

Figures 6, 7 and 8 depict the behavior of the frequencies corresponding to the lowest eighteen modes for a suspended cable possessing the physical properties defined in Table 1. Figures 6 to 8 refer respectively to suspension inclinations of $\theta = 0^0$ (horizontal), 30^0 and 60^0. The results shown there independently confirm the findings of Bliek (1984) and a Triantfyllou (1984b) that in a strict sense, frequency crossover of the in-plane modes occurs only for the special case of horizontally suspended cables (Fig. 6), whereas nonzero inclinations lead to a glancing (hybrid) behavior of the frequency plots (Figs. 7 and 8). These computations employed the method developed by Rosenthal (1981) which was described earlier in the report.

In each of the figures the horizontal axis depicts the sag-to-length ratio which ranges from near zero for taut cables to slightly over one-half for a completely slack or doubled-up cable whose end positions are made to coincide ("slightly over one-half" because of the stretch induced by the cable's weight). All inplane mode curves (which coincide with out-of-plane mode curves over certain ranges) are shown as solid lines. Dashed lines depict ranges over which only out-of-plane modes exist. The chord-to-length ratios corresponding to these sag-to-length ratios are also indicated and range from slightly greater than one for a tautly stretched cable to zero for the doubled-up case.
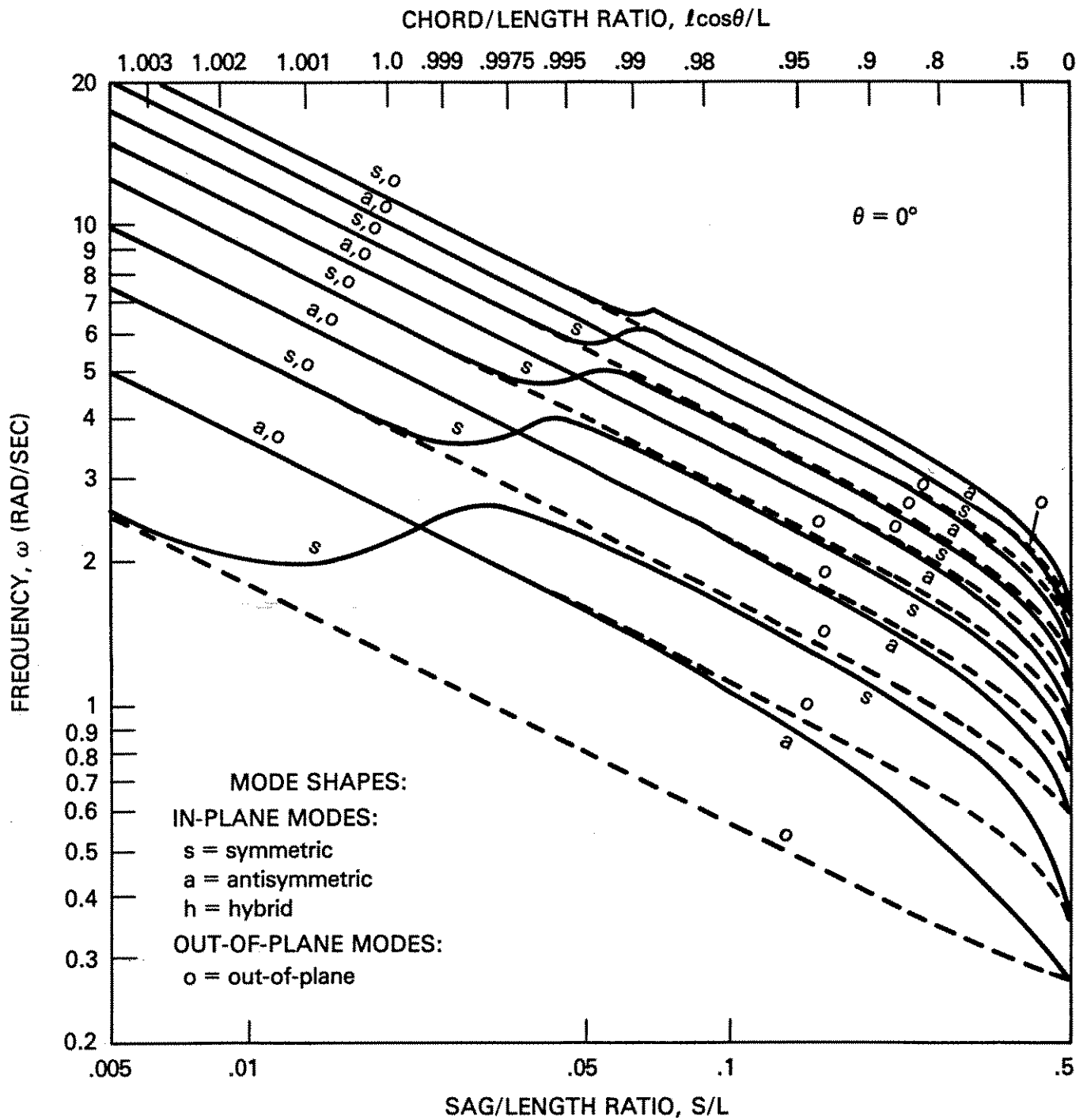
Figure 6 - Natural frequencies for a horizontal (θ = 0) extensible cable in air as a function of the ratio of cable sag to length, s/L. Cable properties as in Table 1.

The vertical scale denotes the frequency ω of all the depicted modes in radians per second. Both the horizontal (sag/length) and vertical scales are logarithmic to show the full ranges of values. Except for very large sag and for the cross-over effects (or the comparable hybrid mode transition for the inclined cases), these logarithmic frequency plots all exhibit a distinct downward slope equal to $-1/2$. This is because the frequency is approximately proportional to the square root of the horizontal tension component H_1, while the tension itself is approximately proportional to the sag.

Since the horizontally-suspended cable is a limiting special case of suspension at an arbitrary angle of inclination, the following discussion will be limited to the behavior of frequency with sag as shown in Fig. 8, the case of $\theta = 60°$ inclination. In this figure we focus our attention respectively on the lowest out-of-plane and the lowest in-plane modes, since higher pairs of such modes possess characteristics which are similar to those of the lowest pair.

We note that the lowest out-of-plane mode has a frequency which is remarkably linear with sag, even out to the maximum sag of slightly over one-half. This mode is the only one which exhibits this high degree of linearity. The corresponding in-plane frequency at the low-sag end begins to rise above the out-of-plane value and initially continues to exhibit an essentially symmetric mode shape. This is the well-known lowest resonance of

a taut string. As its frequency rises towards the frequency of the second out-of-plane mode, however, it loses its symmetry, becoming "hybrid" as Bliek and Triantfyllou termed it.

As its frequency glances from the second in-plane mode frequency (touching it in the horizontal case), it then remains only sightly below the second out-of-plane mode, becoming decidely anti-symmetric with increasing sag. For higher values of sag, the first in-plane mode then lowers its frequency away from the second out-of-plane value, and finally returns to where the lowest pair again has two identical frequencies, which correspond to the pair of orthogonal pendulum modes at maximum sag, i.e. a cable folded back along its length. The figure shows the corresponding behavior for all of the nine pairs of out-of-plane and in-plane modes which were computed as part of this study.

Bliek (1984) has compared results from the perturbation theory (Triantafyllou, 1984) with a finite-difference solution for the linear cable dynamics. An explicit centered-difference scheme was selected to solve the problem by means of a transfer matrix formulation. From the numerical simulation, which can be considered as "exact", predictions of the dynamic tension, angle of inclination, and tangential and normal displacements can be obtained. The natural frequencies are dependent upon three parameters:
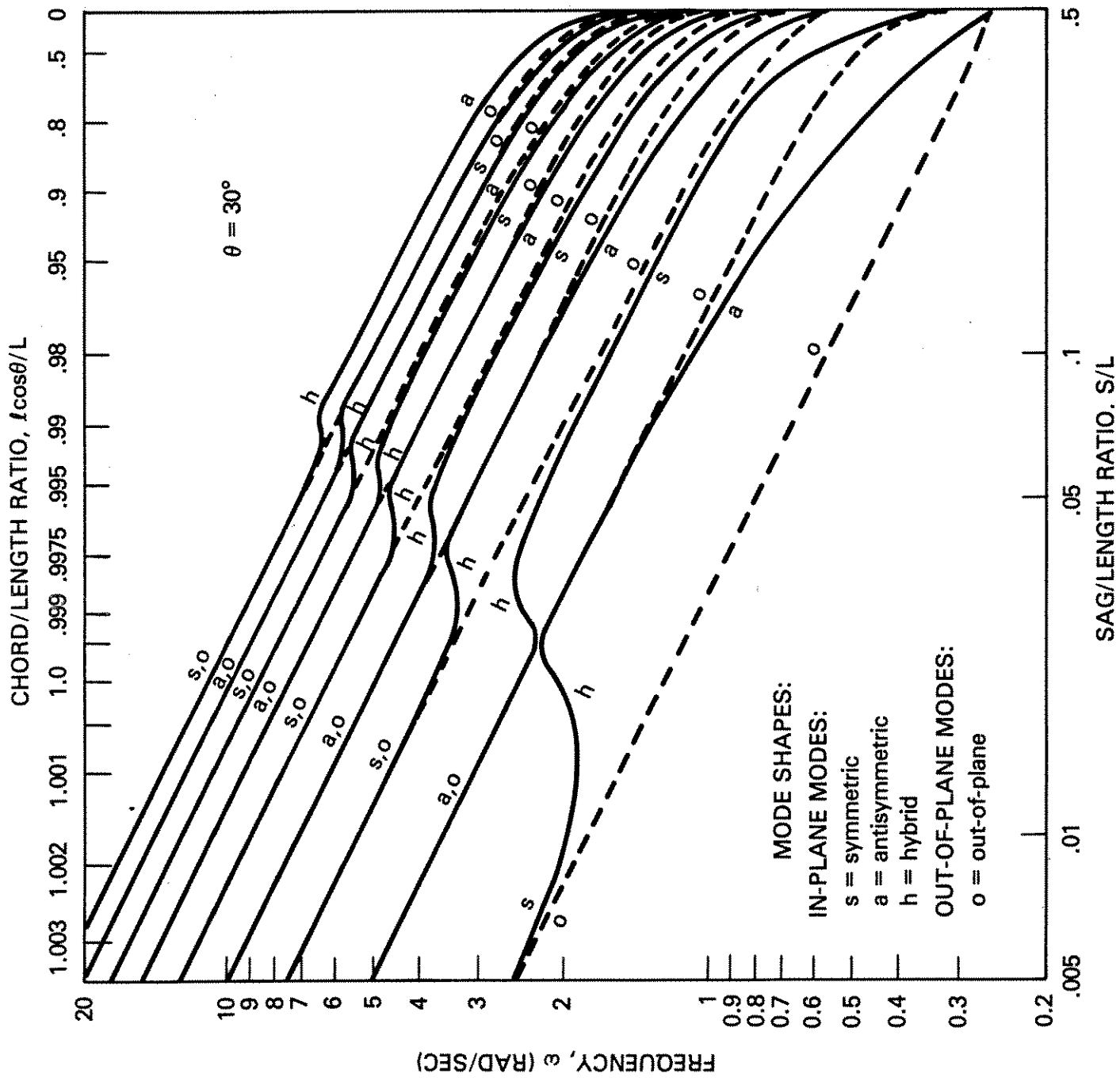
Figure 7 - Natural frequencies for an inclined ($\theta = 30^0$) extensible cable in air as a function of the ratio of cable sag to length, s/L. Cable properties as in Table 1.

MODE SHAPES:

IN-PLANE MODES:
s = symmetric
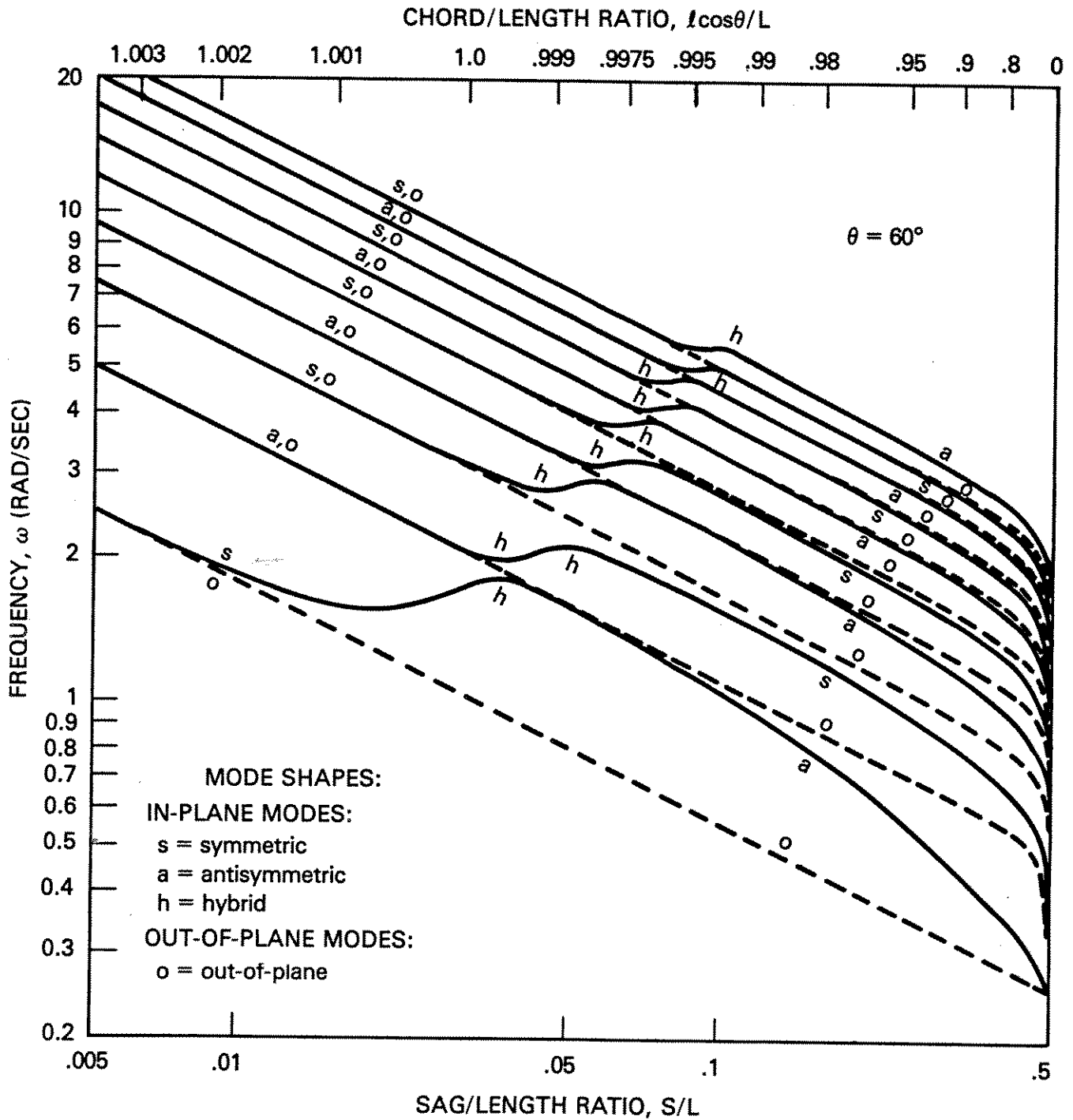a = antisymmetric
h = hybrid

OUT-OF-PLANE MODES:
o = out-of-plane

Figure 8 — Natural frequencies for an inclined ($\theta = 60^0$) extensible cable in air as a function of the ratio of cable sag to length, s/L. Cable properties as in Table 1, legend as in Figures 6 and 7.

o the inclination angle, θ_a:

o the non-dimensional weight, mgL/H_1.

o and, the elastic strain, H_1/EA.

Here H_1 is the tension component $H/\cos\theta_a$. The latter two can be combined as shown earlier into the single fundamental parameter λ^2 that characterizes the cable dynamics. As noted earlier, λ^2 is proportional to the ratio of the elastic stiffness to the catenary stiffness.

Some typical examples of the results obtained for an extensible cable in air by Bliek are shown in Figs. 9 to 11. A value of $(H_1/EA)^{-1} = 400$ was employed in the calculations. This is representative of a steel cable where the ratio of the elastic, or longitudinal, and transverse wave speeds is $c_{el}/c_{tr} = 20$. The numerical results were obtained with a centered difference scheme using 100 integration intervals over the length of the cable.

The natural frequencies of the first two symmetric and antisymmetric transverse modes are plotted in non-dimensional form as a function of mgL/H_1 for a horizontal cable ($\theta = 0^0$) and for an inclined cable ($\theta = 30^0$). The modal crossover is clearly shown for the horizontal cable in Fig. 9 and the perturbation theory and numerical results are in overall good agreement. When the cable is inclined at $\theta = 30^0$ there no longer is a frequency crossover, but rather the hybrid mode transition as shown in Fig. 10. The symmetric modes are transformed into antisymmetric modes and vice versa as shown earlier in Fig. 5. Again there is
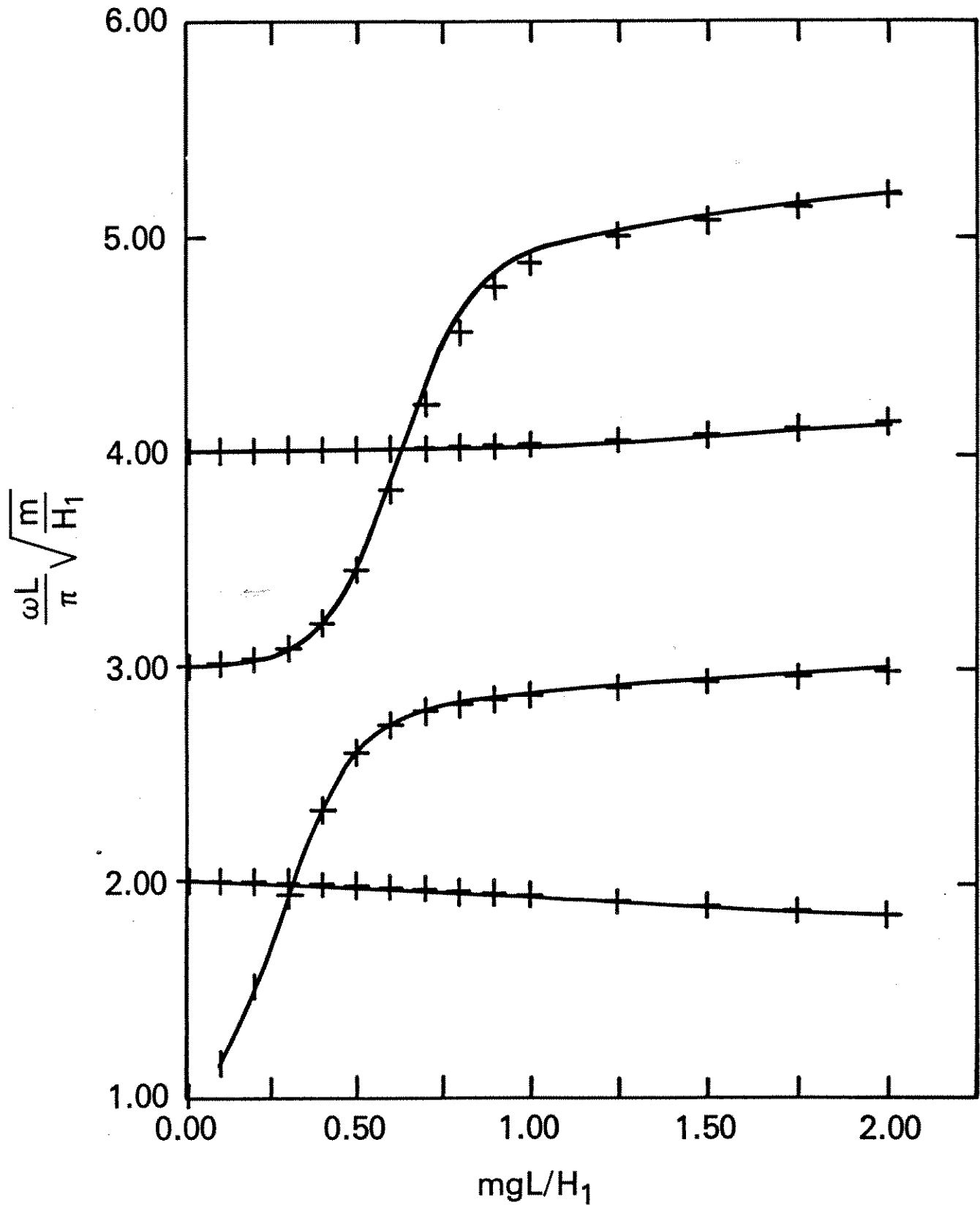
Figure 9 – Natural frequencies for the first two symmetric and antisymmetric modes of an extensible cable in air as a function of the non-dimensional weight parameter, mgL/H_1: from Bliek (1984). Horizontal cable, $\theta = 0^0$, $(H_1/EA)^{-1} = 400$. Asymptotic theory, ——— ; numerical simulation, +.

good agreement between the perturbation solution and the numerical simulation. The natural frequencies for the first pair of modes are shown on an expanded scale in Fig. 11. This enlargement demonstrates very clearly that no crossover exists. This hybrid modal transition now has been demonstrated conclusively by applying the perturbation solution (Triantafyllou, 1984b: Bliek, (1984) and by means of independent numerical simulations by Bliek and the present writers.

The results in Figs. 9 to 11 show the overall good agreement between the two solution approaches. However, at large inclination angles ($\theta \sim 60^0$) and the very high values of the non-dimensional weight mgL/H_1 the perturbation solution diverges from the numerical simulation (Bliek, 1984). The agreement between the two approaches improves at the higher cable modes where the change in cable tension becomes smaller over a wavelength of the vibration.

6. SLACK CABLES WITH ATTACHED MASSES

All of the results discussed thus far have been limited to horizontal and inclined bare cables. However, there are many marine applications where cables have arrays of instrumentation modules, weights and buoyancy elements attached to them. The computer code NATFREQ was developed at the California Institute of Technology for the Naval Civil Engineering Laboratory to provide a means for predicting the natural frequencies, mode

mass term affects only the transverse motions of the cable (in-plane and out-of-plane) and not the longitudinal or tangential motions. Thus in order to derive a complete dynamic analysis of a slack cable in water the natural frequencies of the transverse modes must be corrected for the added mass effect of the fluid. The elastic or tangential modes need not be corrected for the fluid inertia or added mass. The mass of attached discrete elements such as the cylindrical lumps discussed in the previous section also must be corrected for the fluid inertia effect.

The dimensionless added mass coefficient C_{am} is defined by

$$\frac{m_W}{m_A} = 1 + C_{am}/S \tag{26}$$

where m_W is the virtual (physical + added) mass in water, m_A is the mass in air, and S is the specific gravity of the cable or attached member. For a _taut_ cable the natural frequencies in the two media follow the relation

$$\frac{\omega_A}{\omega_W} = \left(\frac{m_W}{m_A}\right)^{1/2} . \tag{27}$$

Then the added mass coefficient is given by

$$C_{am} = S \left(\frac{\omega_A}{\omega_W}\right)^2 - 1 . \tag{28}$$

and C_{am} can be derived from measurements of the natural frequencies in air and in water. Ramberg and Griffin (1977) have reported extensive measurements of the added mass of marine cables by this method for the case of taut cables. Less extensive measurements by Ramberg and Griffin of the natural frequencies of slack marine cables in the two media suggested that the added mass contribution was the same for slack and taut cables when the static effect of buoyancy on λ^2 was properly accounted for in the crossover or hybrid response regime. In most instances it is reasonable to assume that $C_{am} = 1$; that is, the added mass is equal to the volume of fluid displaced by the cable or attached mass.

Hydrodynamic Drag   An important consequence of the resonant cross flow oscillations of structures and cables due to vortex shedding is an amplification of the mean in-line drag force (or equivalently the drag force coefficient C_D). The drag amplification measured prior to 1980 under a variety of conditions has been reported by Griffin et al (1981). More recent and extensive measurements of the drag on cables and cylinders in water are discussed by Vandiver (1983), Griffin and Vandiver (1983) and Griffin (1985). From all of these discussions it is clear that vortex-excited vibrations of cables and cylinders in water can cause amplifications in the hydrodynamic drag of up to 250 percent.

Two crucial elements in the accurate prediction of the hydrodynamic drag on a vibrating cable are accurate estimates of the natural frequencies and the mode shapes associated with the vibrations. The frequency must be known in order to determine whether the Strouhal frequency of vortex shedding will lock-on or resonate with one or several of the natural frequencies of the cable. The mode shape must be known in order to determine the vortex-excited strumming pattern along the cable. Then the local cross flow displacement amplitude distribution lengthwise along the cable can be used to predict the overall hydrodynamic drag from the local drag amplification.

The NATFREQ computer code described by Sergev and Iwan (1980) by Griffin and Vandiver (1983) has the capability to predict the strumming drag on a taut cable with or without attached masses. In order to make a comparable strumming assessment for a slack cable configuration, the natural frequencies and mode shapes also must be known with some accuracy. The methods described by Triantafyllou (1984), Bliek (1984), and in this report can be applied to the case of a bare cable. For a slack cable with attached masses, the SLACK1 and/or SLACK2 computer codes can be used to predict the in-plane natural frequencies and mode shapes which are influenced by the cable strumming. The results discussed in the previous section clearly show that for slack cables, accurate predictions are limited to the lowest cable modes. Otherwise only a rough approximation is

possible. This is in contrast to the NATFREQ code, for which Sergev and Iwan give an example showing the computed 162nd mode for a 4700 m (15400 ft) long taut cable with 380 attached masses.

8. SUMMARY

   Conclusions. The linear theory for the dynamics of horizontal cables with sag-to-span ratios of 1:8 or less can be described by the linear solution derived by Irvine and Caughey (1974). This is a special case of the more general perturbation solution for the linear dynamics of taut and slack cables derived by Triantafyllou (1984b) and Bliek (1984). The dynamics of horizontal slack cables are characterized by a frequency "crossover" behavior. This modal crossover is a complex phenomenon whereby three modes of the cable have the same natural frequency. These modes include a symmetric in-plane mode, an antisymmetric in-plane mode and an out-of-plane or sway mode.

   A frequency crossover never occurs in the case of the inclined cable. Instead the modes are hybrid in form over the transition range from the taut to the inextensible cable behavior. These natural modes are a mixture of symmetric and antisymmetric modes as shown by Triantafyllou (1984b) and in this report. There are virtually no differences in the natural frequencies computed by the methods of Triantafyllou and Irvine (1978), but the mode shapes of the inclined slack cable are unique in form as the natural frequencies pass close together but

never cross over. Several examples of both the crossover and the hybrid mode behavior are given in this report.

The results obtained in this study have shown that for slack cables with attached masses only the lowest cable modes can be modelled with reasonable accuracy at the present time. Otherwise only a rough approximation is possible. This is because of the relatively small numbers of finite elements and integration intervals which limit the present capabilities of the two codes. The addition of attached masses to the bare cable affects both the antisymmetric and symmetric in-plane modes. There is a systematic increase in the natural frequencies of a slack cable as masses are attached to it. For the symmetric modes the natural frequency may increase or decrease, depending upon the proximity to the crossover or hybrid regions of the cable response. This is caused by the extreme sensitivity of the symmetric cable modes to small changes in tension and sag near those regions.

Recommendations. The capabilities of existing computer codes are limited, as mentioned above, to calculating with accuracy only the lowest cable natural frequencies and mode shapes. The computations of the higher modes are rough approximations because of the relatively small number of finite elements or integration intervals that can be employed efficiently on all but the largest computers. In order to make practical engineering calculations of the dynamics of slack

cables with attached masses, more efficient solution routines and means to employ the capabilities of existing medium size and large-scale computing machines must be sought. The approach of Rosenthal (1981) based upon Stodola's method of successive approximations appears to be the more promising one for the case of a cable with attached masses. Then the need to solve the large matrix equations inherent in the finite element method is eliminated, and the computational resources are greatly reduced.

For a bare cable either of the approaches described by Irvine and Caughey (1974), Triantafyllou (1984b) or Bliek (1984), or some combination of the three, should yield positive results. Rosenthal's approach also is applicable to the special case of the bare cable as shown previously and in this report.

The effects of added mass or fluid inertia are an important consideration for the transverse (in-plane and out-of-plane) modes of a cable in water. The longitudinal or elastic modes are unaffected by the added mass of the fluid. Thus any improved and more "user friendly" slack cable dynamics computer code should account for the added mass effect on both the cable and any discrete masses which are attached to it.

Two crucial elements in the accurate prediction of the hydrodynamic drag on a vibrating marine cable are accurate estimates of the natural frequencies and mode shapes of the vibrations. This and other recent studies have demonstrated the complexity of the slack cable dynamics problem. Thus an

assessment of the strumming behavior of a slack cable and of the overall hydrodynamic drag presently is limited to the lowest cable modes as described earlier. It is recommended that any improved slack cable dynamics code also include the capability of predicting the hydrodynamic drag. A similar capability is available in the taut cable dynamics code NATFREQ described by Sergev and Iwan (1980).

9. ACKNOWLEDGEMENTS

10. REFERENCES

A. Bliek, 1984, "Dynamics of Single Span Cables", Ph.D. Thesis, Massachusetts Institute of Technology.

M.L. Gambhir and B. de V. Batchelor, 1978, "Parametric Study of the Free Vibration of Sagged Cables", Computers & Structures, Vol. 8, 641-648.

O.M. Griffin, 1985, "Hydrodynamic Loads on Marine Risers and Cables Due to Vortex Shedding", NRL Memorandum Report, in preparation.

O.M. Griffin and J.K. Vandiver, 1983. "Flow-Induced Vibrations of Taut Marine Cables with Attached Masses", Naval Civil Engineering Laboratory Report CR 84.004; see also 1984. Transactions of the ASME, Journal of Energy Resources Technology, Vol. 106, forthcoming.

O.M. Griffin, S.E. Ramberg, R.A. Skop, D.J. Meggitt and S.S. Sergev, 1981, "The Strumming Vibrations of Marine Cables: State of the Art", Naval Civil Engineering Laboratory Technical Note N-1608.

W.M. Henghold and J.J. Russell, 1976, "Equilibrium and Natural Frequencies of Cable Structures (A Nonlinear Finite Element Approach)", Computers and Structures, Vol. 6, 267-271.

W.M. Henghold, J.J. Russell and J.D. Morgan, 1977, "Free Vibrations of a Cable in Three Dimensions, Proceedings of the ASCE, Journal of the Structural Division, Vol. 103, 1127-1136.

H.M. Irvine, 1978, "Free Vibrations of Inclined Cables", Proceedings of the ASCE, Journal of the Structural Division, Vol. 104, 343-347.

H.M. Irvine, 1981, Cable Structures, MIT Press: Cambridge.

H.M. Irvine and T.K. Caughey, 1974, "The Linear Theory of Free Vibrations of a Suspended Cable", Proceedings of the Royal Society of London, Series A, Vol. 341, 299-315, 1974· see also California Institute of Technology Dynamics Lab Report DYNL-108.

W.D. Iwan and N.P. Jones, 1984, "NATFREQ Users Manual - A Fortran IV Program for Computing Natural Frequencies, Mode Shapes and Drag Coefficients for Taut Strumming Cables with Attached Masses and Spring-Mass Combinations", Naval Civil Engineering Laboratory Report CR 84.026.

J.C. McGlothlin, 1982, "Drag Coefficients of Long Flexible Cylinders Subject to Vortex Induced Vibrations", M.S. Thesis, MIT Ocean Engineering Department.

A.G. Pugsley, 1949, "On the Natural Frequencies of Suspension Chains", Quarterly Journal of Mechanics and Applied Mathematics, Vol. 2, 412-418.

S.E. Ramberg and O.M. Griffin, 1977, "Free Vibrations of Taut and Slack Marine Cables", Proceedings of the ASCE, Journal of the Structural Division, Vol. 103, 2079-2092.

S.E. Ramberg and C.L. Bartholomew, 1982, "Vibrations of Inclined Slack Cables", Proceedings of the ASCE, Journal of the Structural Division, Vol. 108, 1662-1664.

J.H. Rohrs, 1851, "On the Oscillations of a Suspension Chain", Transactions of the Cambridge Philosphical Society, Vol. 9, Part 3, 379-398.

F. Rosenthal, 1981, "Vibrations of Slack Cables with Discrete Masses", Journal of Sound and Vibration, Vol. 78, 573-583.

E.J. Routh, 1955, Advanced Dynamics of Rigid Bodies, Sixth Edition, Dover: New York; original published in 1868.

D.S. Saxon and A.E. Cahn, 1953, "Modes of Vibration of a Suspended Cable", Quarterly Journal of Mechanics and Applied Mathematics, Vol. 6, 273-285.

S.S. Sergev and W.D. Iwan, 1980, "The Natural Frequencies and Mode Shapes of Cables with Attached Masses," Naval Civil Engineering Laboratory Technical Note N-1583; see also 1981, Transactions of the ASME, Journal of Energy Resources Technology, Vol. 103, 237-242.

A. Simpson, 1966, "Determination of the inplane natural frequencies of multispan transmission lines by a transfer matrix method", Proceedings of the Institution of Electrical Engineers, Vol. 113, 870-878.

R.A. Skop and G.J. O'Hara, 1970, "The method of imaginary reactions: a new technique for analyzing cable systems", Marine Technology Society Journal, Vol. 4, 21-30.

R.A. Skop and F. Rosenthal, 1982, "Method of Imaginary Reactions for Taut Cables", Proceedings of ASCE, Journal of the Structural Division, Vol. 108, No. ST7, 1669-1671.

A. I. Soler, 1970, "Dynamic response of a single cable with initial sag", Journal of the Franklin Institute, Vol. 290, 377-387.

W.T. Thomson, 1965, Vibration Theory and Applications, Prentice Hall: Englewood Cliffs, NJ; see Chapter VII.

M.S. Triantafyllou, 1982, "Preliminary Design of Mooring Systems", Journal of Ship Research, Vol. 26, 25-35.

M.S. Triantafyllou, 1984a, "Linear Dynamics of Cables and Chains", The Shock and Vibration Digest, Vol. 16, No. 3, 9-17.

M.S. Triantafyllou, 1984b, "The Linear Dynamics of Taut Inclined Cables", Quarterly Journal of Mechanics and Applied Mathematics, Vol. 37, 421-440.

M.S. Triantafyllou and A. Bliek, 1983, "The Dynamics of Inclined Taut and Slack Marine Cables", Offshore Technology Conference Preprint OTC 4498.

A.S. Veletsos and G.R. Darbre, 1983, "Free Vibrations of Parabolic Cables", Proceedings of the ASCE, Journal of Structural Engineering, Vol. 109, 503-519.

H.H. West, L.F. Geschwindner and J.E. Suhoski, 1975, "Natural Vibrations of Suspension Cables", Proceedings of the ASCE, Journal of the Structural Division, Vol. 101, 2277-2291.

H.H. West, J.E. Suhoski and L.F. Geschwindner, 1984, "Natural Frequencies and Modes of Suspension Bridges", Proceedings of the ASCE, Journal of Structural Engineering, Vol. 110, 2471-2486.
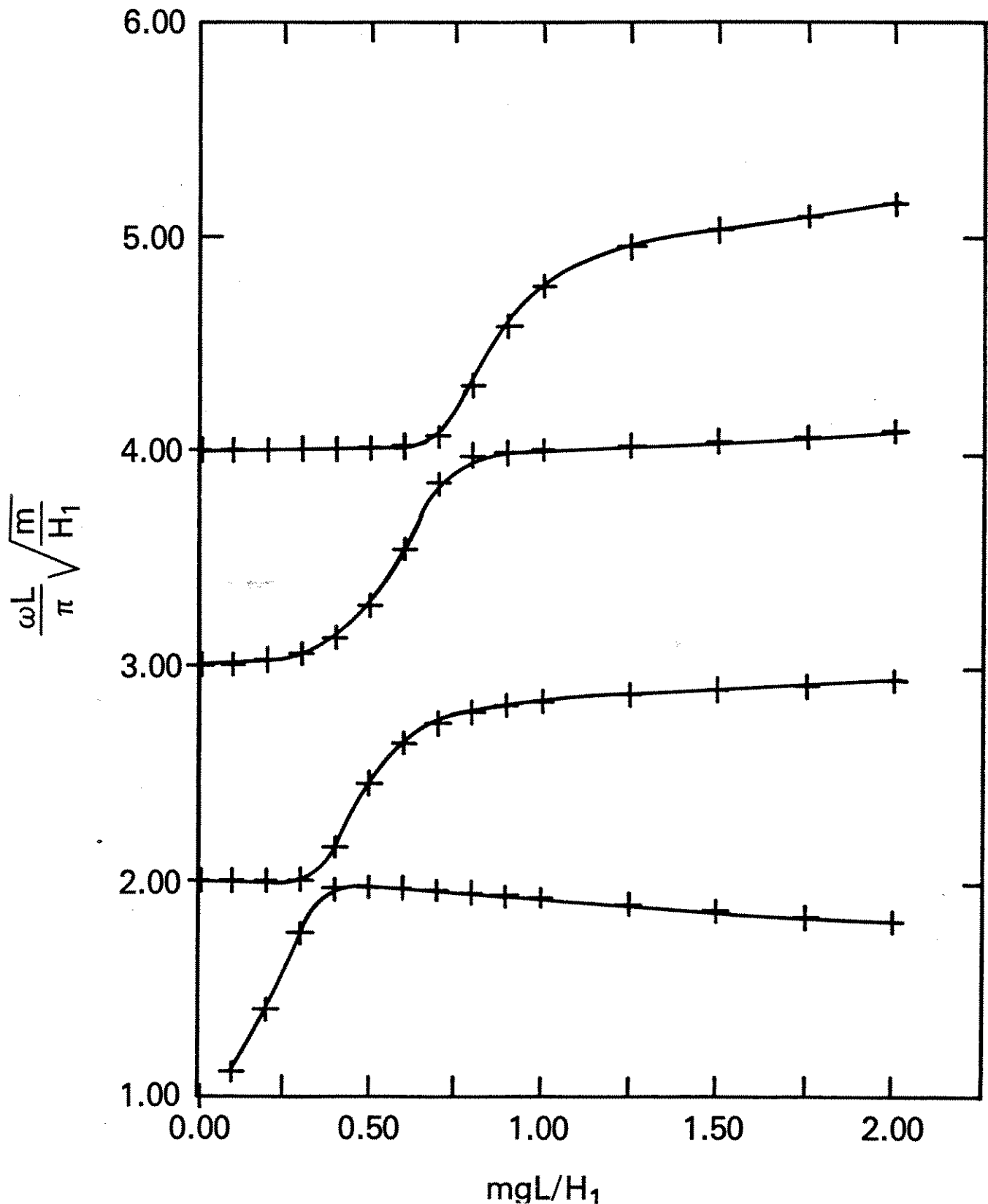
Figure 10 – Natural frequencies for the first two symmetric and antisymmetric modes of an extensible cable in air as a function of the non-dimensional weight parameter, mgL/h$_1$: from Bliek (1984). Conditions as in Figure 9 except that the inclination angle θ = 30⁰.
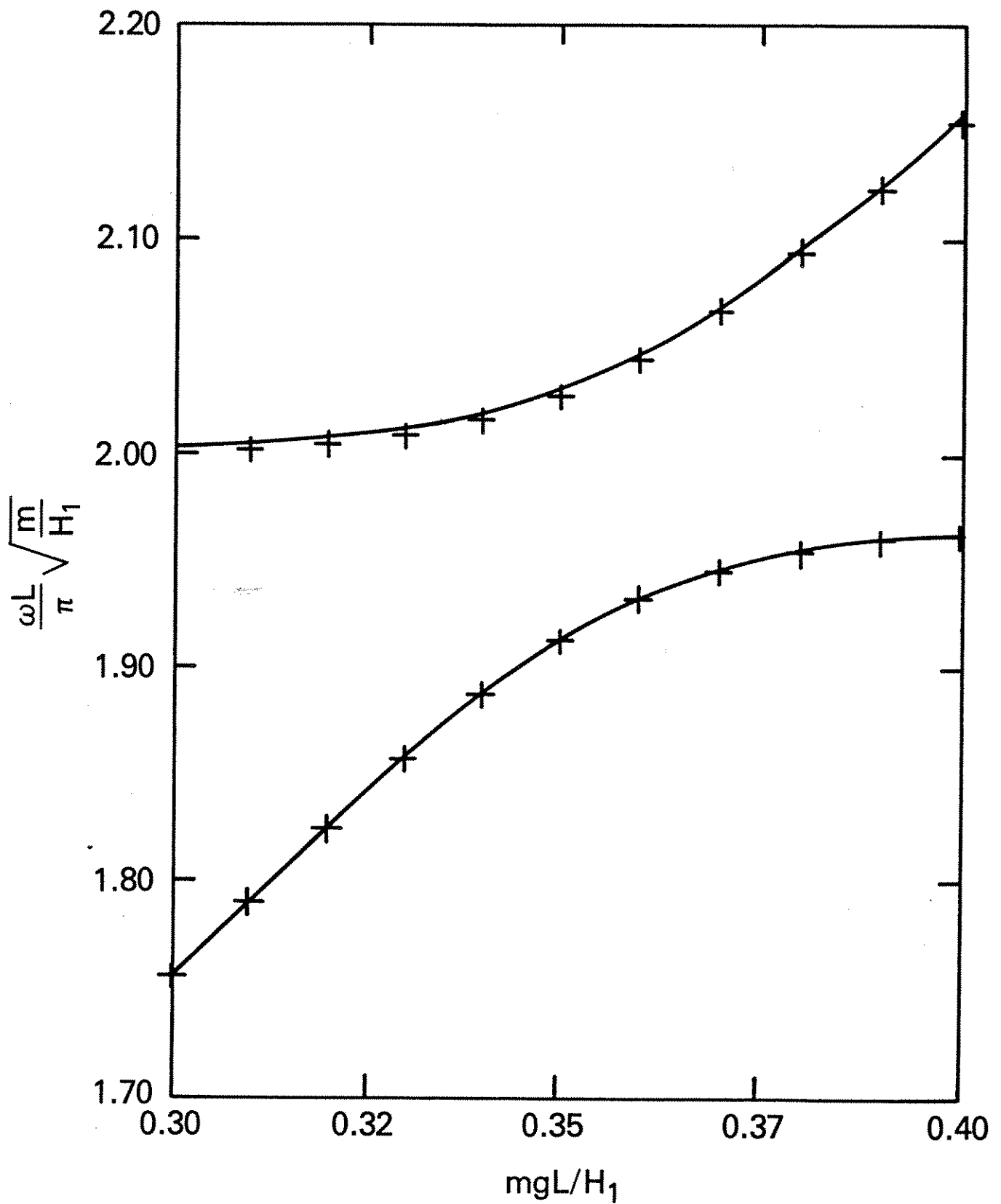
Figure 11 - An expanded plot of the hybrid modal transition zone for the first symmetric and anti-symmetric modes in Figure 10.

shapes and drag coefficients for taut cables with large numbers of attached discrete masses. A basic description of the code and an operating manual to aid in its use are available· see Sergev and Iwan (1980), and Iwan and Jones (1984), respectively. An extensive program of field experiments was conducted to benchmark the capabilities of the NATFREQ code, and a comparison of the code predictions and the results of the experiments has been given by Griffin and Vandiver (1983, 1984).

In this section of the report a comparison is presented of two computer codes which have been developed for predicting the natural frequencies and mode shapes of slack cables with arrays of discrete masses attached to them. This is a preliminary assessment since the capabilities of the codes presently are not as extensive and well-documented as are those of the taut-cable code NATFREQ, and the solution algorithms for the slack cable dynamics are far more complex than are those required for the analysis of taut cables.

The two slack cable codes discussed here are called SLACK1 and SLACK2, respectively. SLACK1 is essentially the three-dimensional cable dynamics code which was developed by Henghold, Russell and Morgan (1977) and modified later at NRL. The finite element formulation employed in SLACK1 is described in detail by Henghold and Russell (1976). Three-node elements are employed in the code which is capable of accommodating up to sixty nodes along the length of the cable. SLACK2 is the most recent version

of the three-dimensional cable dynamics code developed at NRL by Rosenthal (1981). This latter code uses a modified form of the method of imaginary reactions described by Skop and O'Hara (1970) and by Skop and Rosenthal (1982) to obtain the static cable configuration. Then Stodola's method (see Thomson, 1965) is used to calculate the cable dynamics. Stodola's method is a successive approximation approach to computing the natural frequencies and mode shapes of the cable. The use of Stodola's method eliminates the need to solve the large matrix equations which are inherent in the finite element method of computing the natural frequencies. Up to sixty integration intervals can be included over the length of the cable at the present time. Details of the computational scheme are given by Rosenthal (1981). Both computer codes are capable of predicting the out-of-plane and in-plane components of the cable dynamic response. The present discussion is limited to the transverse component of the response since the longitudinal, or elastic, component occurs at higher frequencies and is smaller by an order-of-magnitude.
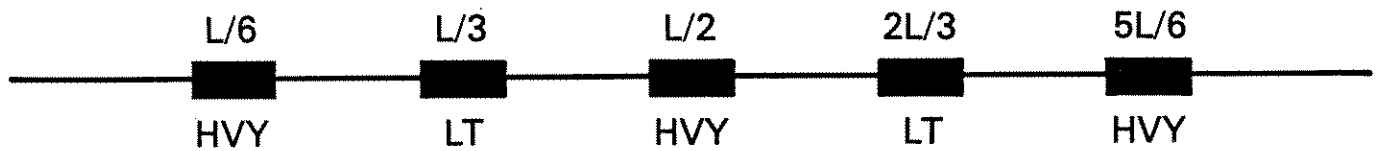
The cable configurations chosen for the comparison and demonstration are slack cable analogues to the taut cable field test set-up which was employed in the NATFREQ code validation. At the test site a 22.9m (75 ft) long by 3.2 cm (1.25 in) diameter taut cable was employed, so that for the present computations the chord length was set equal to $\ell = 22.9$ m (75 ft). The attached masses were cylindrical lumps of PVC into

which lead inserts could be put in order to change the physical mass from "light" ($m = 2$ kg or 4.4 lb_m) to "heavy" ($m = 4.5$ kg or 10 lb_m). In the computations discussed below the cylindrical masses are treated as point concentrated loads. This approximation also is made in the NATFREQ taut cable code. Complete descriptions of the cable, the attached masses, and the test setup and instrumentation are given by McGlothlin (1982) and by Griffin and Vandiver (1983). The two configurations chosen for the computations are shown in Fig. 12. The first consists of two evenly-spaced heavy masses. The second consists of five evenly-spaced masses -- two light cylinders and three heavy cylinders. The cable had a mass per unit length $m = 1.14$ kg/m (0.77 lb_m/ft) in air and an elastic stiffness EA = 8.9 x 10^5N (2×10^5 lb).

Since the relative capabilities of the two codes were not known for the case when masses were attached to the cable, a baseline comparison was made using just the bare cable. Then the relative accuracies can be compared with the results obtained by Rosenthal (1981). The present results are given in Table 2 for the first nine cable modes. Twelve elements and twenty-five nodes were used for the SLACK1 finite element computations while for the SLACK2 computations by Stodola's method thirty integration intervals were used. These conditions were thought to be reasonably comparable. The two methods give estimates of the natural frequencies, in the proper order, which differ by less than five percent for the first nine cable modes. For higher

Figure 12 — Two attached mass/cable configurations employed in
the comparison between the SLACK1 and SLACK2 computer codes. The
configurations shown are taken from the field test report of
Griffin and Vandiver (1983).

modes the estimated frequencies diverge rapidly due to the relatively limited number of elements used. The maximum permissible number of finite elements is dependent on the magnitude of the relative elastic stiffness $AE/mg\ell$, due to the nature of the governing equations for the natural frequencies and the matrix manipulation routines that are used in the SLACK1 code.

The static solutions obtained by the two methods for all of the slack cable configurations are virtually indistinguishable, both for the bare cable and the cable with attached masses. The maximum sag-to-length ratios, s/L, obtained by the two approaches are compared in Tables 2, 3 and 4. These and the comparisons which follow are for a cable deployed in air where added mass effects are not important. A brief discussion of the effects of added mass on the natural frequencies of a slack marine cable is given in the next section of the report.

The natural frequencies obtained for the two cable-attached mass configurations are compared in Tables 3 and 4. The results for the cable with two evenly-spaced attached masses are listed in Table 3 for the first nine natural cable modes. Eighteen finite elements were employed for the SLACK1 computations, while two cases of fourteen and thirty integration intervals were employed for SLACK2. In each case the sequence of modes was properly ordered, i.e. out-of-plane, antisymmetric, etc. The mode order shown is typical of relatively large sag-to-length

TABLE 2

Natural Frequencies of Horizontal Slack Cables
(No Attached Masses)

Uniform Cable, $AE/mg\ell$ = 3500; Chord-to-Length, ℓ/L = 0.987

O, A, S = out-of-plane, in-plane antisymmetric and symmetric modes

	Frequency, ω (rad/sec)	
	SLACK1	SLACK2
	Finite elements	Stodola's method
Mode Type	(12 elements, 25 nodes)	(30 integration intervals)
O	2.706	2.706
A	5.317	5.282
O	5.421	5.389
S	7.728	7.612
O	8.160	8.060
A	10.971	10.660
O	10.983	10.710
S	13.584	12.970
O	13.884	13.332
Maximum sag-to-length, s/L =	0.0716	0.0714

ratios to the right of the modal crossover or hybrid mode region. For this condition the cable exhibits largely inextensible behavior; that is, λ^2 is large. For the cable deployed during the field tests, $\lambda^2 \tilde{=} 650$ for $\ell/L = 0.987$ and $EA/mg\ell = 3500$.

It can be seen from Table 3 that the results obtained with the two computer codes for the cable with attached masses differ more than the comparable bare cable results. The out-of-plane first mode frequency computed using SLACK1 is ten percent higher than the same frequency computed using SLACK2. The solutions obtained with the two codes diverge still further until for the ninth mode the SLACK1-predicted frequency is eighteen percent higher than the SLACK2 prediction. When the number of integration intervals is reduced by one-half, there is only a three percent decrease in the SLACK2 prediction of the ninth-mode frequency. It was found in an earlier study (Rosenthal, 1981) that the SLACK1 code predictions tended to overestimate the higher mode frequencies due to artificial stiffness effects upon the finite element solution when the number of elements was too few. Conversely, the SLACK2 prediction tended to underestimate the true natural frequencies when too few integration intervals were used. Thus the predicted frequencies are only true estimates for the lowest cable modes. When the number of finite elements or integration intervals is of the order of the mode number, the predicted frequencies are only rough approximations.

TABLE 3

Natural Frequencies of Horizontal Slack Cables
(Two Attached Masses)

Uniform Cable, AE/ $mg\ell$ = 3500; Chord-to-Length, ℓ/L = 0.962

O, A, S = out-of-plane, in-plane antisymmetric and symmetric modes

Frequency, ω (rad/sec)

Mode Type	SLACK1 Finite elements (18 elements, 37 nodes)	SLACK2 Stodola's method (30 intervals)	(14 intervals)
O	2.231	2.021	2.020
A	4.172	3.688	3.674
O	4.416	3.877	3.861
S	7.251	7.038	6.959
O	7.496	7.357	7.271
A	8.969	8.349	8.205
O	9.150	8.464	8.312
S	11.043	9.675	9.408
O	11.361	9.821	9.547
Maximum sag-to-length, s/L =	0.120	0.119	0.118

The natural frequencies for the cable with five attached masses are compared in Table 4. The mode type and ordering of both the SLACK1 and SLACK2-calculated frequencies are correct for all nine modes. However, the frequencies predicted by the SLACK1 code again are consistently higher than the corresponding SLACK2 predictions. The first out-of-plane mode frequency is thirteen percent higher and this difference increases to eighteen percent for the eighth symmetric mode. Once again the static solutions obtained by the two methods are virtually indistinguishable. There is a general increase in the natural frequency of a given mode as the number and mass of the attached bodies are increased. This is opposite to what is found for an extensible taut cable. There also is an increase in the sag-to-length ratio s/L as the attachments on the cable are increased in number.

The first four in-plane mode frequencies for the three cable configurations discussed here are compared in Table 5. It is seen from the results that the increase in frequency is systematic for the antisymmetric modes. For the symmetric modes the natural frequency first increases relative to the bare cable when two equally-spaced masses are attached to the cable. Then the frequency decreases slightly when the number of attached masses is increased to five. This behavior is caused by the extreme sensitivity of the symmetric cable modes to small changes in tension and sag near the crossover or hybrid regions of the

TABLE 4

Natural Frequencies of Horizontal Slack Cables
(Five Attached Masses)

Uniform Cable, $AE/mg\ell = 3500$: Chord-to-length, $\ell/L = 0.962$

O, A, S = out-of-plane, in-plane antisymmetric and symmetric modes

Mode Type	Frequency, ω (rad/sec)	
	SLACK1 Finite elements (18 elements, 37 nodes)	SLACK2 Stodola's method (36 intervals)
O	2.326	2.061
A	4.359	3.832
O	4.624	4.047
S	6.156	5.226
O	6.590	5.506
A	9.025	7.816
O	9.257	7.892
S	10.828	9.172
O	11.402	9.240
Maximum sag-to-length ratio, s/L =	0.122	0.122

cable response. The increase in static tension caused by the addition of the attached masses is given in Table 5 for the three cases.

The shapes of the fourth and eighth symmetric modes for the cable with five attached masses are plotted in Fig. 13. The predictions were made with the SLACK2 code. In each case the vertical scale is normalized by the factor

$$\psi_R = \left[\int_{s=0}^{L} [\psi(s)]^2 dm \right]^{1/2}. \tag{25}$$

The integrand is discontinuous at the locations of the individual attached masses, leading to a Stieltjes integral representation consisting of a regular integral representing the bare cable and a sum of discrete mass terms (Rosenthal, 1981). It is clear from the plotted mode shapes that in general the masses are in motion and do not lie at nodes of the vibration pattern. This is similar to the findings of Griffin and Vandiver (1983,1984) for the case of taut marine cables.

7. ADDED MASS AND HYDRODYNAMIC DRAG

Added Mass. The effect of a dense fluid such as water on the cable dynamics is an important consideration in terms of the added mass, or fluid inertia, component of the hydrodynamic force system. The total, or virtual, mass of the cable in water then is the sum of the physical mass and the added mass. The added

TABLE 5

Natural Frequencies of Horizontal Slack Cables

Uniform Cable, AE/ $mg\ell$ = 3500; Chord-to-Length, ℓ/L = 0.962

A, S = in-plane antisymmetric and symmetric modes

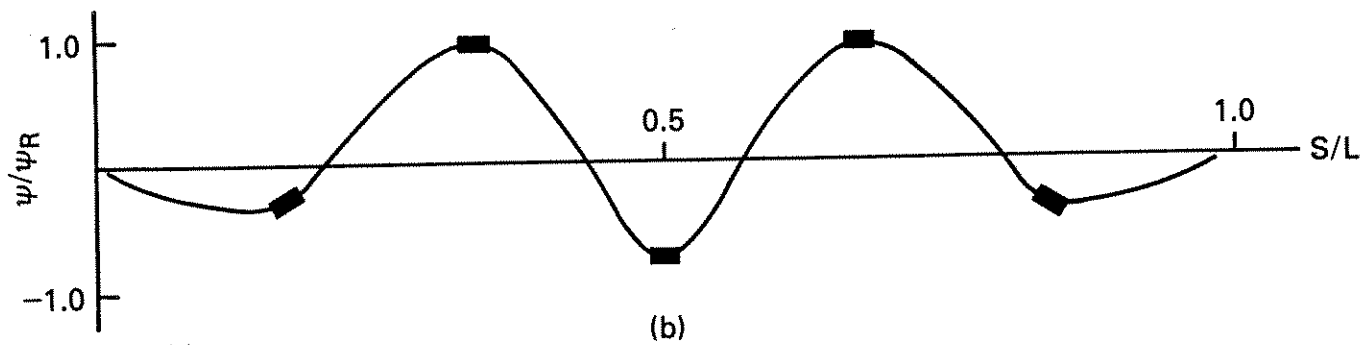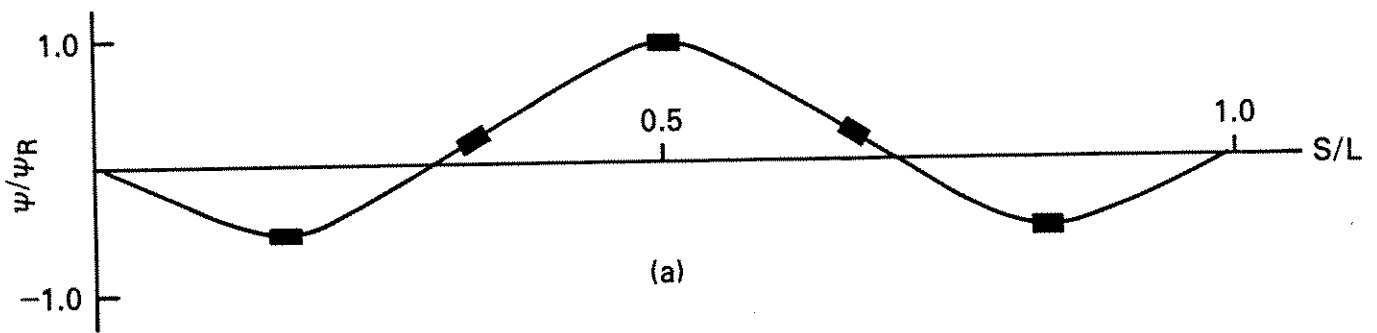| Mode Type	Bare Cable	Frequency, ω (rad/sec) SLACK1 Finite elements (18 elements, 37 nodes) Two, five attached masses	
A	3.890	4.172,	4.359
S	5.834	7.251,	6.156
A	8.157	7.251,	9.025
S	10.190	11.043,	10.828
Maximum sag-to-length, s/L =	0.120	0.120	0.122
Average tension, H/$mg\ell$ =	1.025	1.494	1.766

Figure 13 - Normalized displacement patterns for the first two symmetric modes of the slack cable with five attached masses. Chord-to- length, $\ell/L = 0.962$: elastic stiffness, $AE/mg\ell = 3500$.